Microfluid Nanofluid (2008) 5:551–559
DOI 10.1007/s10404-008-0267-7

RESEARCH PAPER

Thermal interactions in nanoscale fluid flow: molecular dynamics simulations with solid–liquid interfaces

Bo Hung Kim · Ali Beskok · Tahir Cagin

Received: 13 November 2007 / Accepted: 8 February 2008 / Published online: 28 February 2008

Abstract Molecular dynamics (MD) simulations of nano-scale flows typically utilize fixed lattice crystal interactions between the fluid and stationary wall molecules. This approach cannot properly model interactions and thermal exchange at the wall–fluid interface. We present a new interactive thermal wall model that can properly simulate the flow and heat transfer in nano-scale channels. The new model utilizes fluid molecules freely interacting with the thermally oscillating wall molecules, which are connected to the lattice positions with "bonds". Thermostats are applied separately to each layer of the walls to keep the wall temperature constant, while temperature of the fluid is sustained without the application of a thermostat. Two-dimensional MD simulation results for shear driven nano-channel flow shows parabolic temperature distribution within the domain, induced by viscous heating due to a constant shear rate. As a result of the Kapitza resistance, temperature profiles exhibit jumps at the fluid–wall interface. Time dependent simulation results for freezing of liquid argon in a nano-channel are also presented.

Keywords Liquid–solid interface · Molecular dynamics simulations · Kapitza resistance · Nanofluids

B. H. Kim · A. Beskok (✉)
Aerospace Engineering Department, Old Dominion University, Norfolk, VA 23529, USA
e-mail: abeskok@odu.edu

T. Cagin
Chemical Engineering Department, Texas A&M University, College Station, TX 77840, USA

List of symbols

k_b	Boltzmann constant, 1.3806×10^{-23} m^2 kg/s^2 K
N_f	number of fluid molecules
N_w	number of wall molecules
σ	diameter of molecules (zero potential distance between molecules)
r_{ij}	distance between ith and jth molecules
r_0	original position of a wall molecule in a wall lattice crystal
r_i	instantaneous position of a wall molecule in thermal oscillation
τ	characteristic time
ε	depth of Lennard–Jones potential wall
m	mass of molecules
K	crystal bond stiffness
ρ	number density (N/σ^2)
V	interaction potential function
F	interaction force
U_w	velocity of the walls
$\dot{\gamma}$	shear rate
h	distance between the walls (channel width)
$<a>$	ensemble average of $\boldsymbol{a}$ in the system

1 Introduction

In nano-scale flows, molecular structure of the fluid and surfaces, and their interactions between them at the atomistic length scales play a key role, and hence the molecular dynamics (MD) method emerges as a viable approach for investigation of the flow physics in such scales (Priezjev et al. 2005; Karniadakis et al. 2005; Cieplak et al. 1999). Recent developments in MD simulation of the nanoscale fluid flow are summarized in Koplik and Banavar (1995)

and Evans and Hoover (1986). As described in these two review articles, one of the primary interests in the nanoscale fluid flow is the investigation of fluid/surface interactions and their implication on the boundary conditions applicable for continuum level formulations. MD distinguishes itself from other simulation methods by providing atomistic level direct numerical experiments that enable simulations with various physical conditions. Therefore, MD can potentially address such issues as solid–fluid interfaces and interactions arising in the nanoscale-regime.

Previous nanoscale fluid flow MD simulations were focused on velocity slip on the boundary, and they have shown that the boundary slip on the liquid–solid interface is mainly a function of the wall–fluid interaction strength, fluid/wall density and shear rate (Thompson and Troian 1997; Cieplak et al. 2000). Many nanoscale fluid flow simulations had the fluid confined between two walls, and applied periodic boundary conditions in the flow direction. One of our main objectives for this study is an implementation of physically sensible walls that realistically emulate solid–fluid interactions and thermal exchange between solid and the fluid. In most of the earlier simulations, a thermostat is applied to all fluid molecules in order to maintain the system at thermal equilibrium, and hence, the thermal boundary condition on the wall/fluid interface is often tampered by this choice.

In order to describe interactions of gas molecules with the surface, Maxwell (1879) described specular and diffuse reflection models in 1897, which were appropriate in kinetic theory based approaches (Bird 1994). However, many MD simulations use more advanced wall models with fixed lattice structure instead of using simple specular walls. Fixed lattice walls consist of wall molecules fixed in their lattice positions and collide (interact) with fluid molecules via intermolecular forces (Thompson and Troian 1997; Thompson and Robbins 1990) without recoil. This model is similar to specular wall approach in terms of the energy conservation of the fluid confined within the wall boundary. However, it can facilitate application of a shear through the motion of the walls (i.e. changing the position of the wall molecules in every timestep). Similarly, instead of fixing the wall molecules in their lattice positions, it is possible to assign very heavy mass (e.g. $\text{mass}_{\text{wall}} = 10^{10} \times \text{mass}_{\text{fluid}}$) to wall molecules, which allows motion of wall molecules based on their interactions with fluid atoms and each other (Koplik et al. 1989). This enables the system to conserve its total energy, and prevents wall molecules from being swept away during the simulation. Since "fixed" lattice wall model impart energy to the system, it is necessary to utilize a thermostat to dissipate viscous heating induced by the shearing motion.

There are several widely accepted methods of applying thermostats to the model system in MD simulations to maintain the systems at constant temperature. To name a few, Anderson (1980) developed a thermostat using stochastic forces that modify the velocities to maintain average kinetic energy of the molecular system consistent with the equipartition theorem. Berendsen (1984) developed a method that is efficient in relaxing the model system to a desired temperature by coupling an external bath at a constant temperature to the system and modifying the velocities at each iteration through a differential feedback mechanism. This efficient and widely used method though maintained constant temperature thermodynamics state, does not produce canonical probability distribution in momentum space during simulations (Karniadakis et al. 2005). The most popular thermostat that sustains the canonical ensemble distribution both in configuration and momentum space is the Nose–Hoover thermostat, which generates canonical temperature fluctuations by affecting intermolecular forces from extended ensemble system. It was first suggested by Nose (2002, 1984), and then modified by Hoover (1985).

Although, thermostats in the system can be used to maintain isothermal state of the system in equilibrium MD simulations, care should be taken when they are used in steady state simulations where thermal transport and fluid flow is critical. Notably, physically sound approaches should be implemented to model the thermal transport at the wall–fluid interfaces. Sun and Ebner (1992a) utilized a "diffuse reflection" model, which accounted the interactions between the fluid and wall molecules through the use of mathematically smooth walls that reflect fluid molecules with random thermal velocities based on the Maxwell–Boltzmann velocity distribution. However, with the authors' candid admission this model could only be a crude approximation of real physics at the wall/fluid interface. In order to improve their model, Sun and Ebner developed an advanced "diffuse reflection" wall model (Sun and Ebner 1992b), which reflected both fluid and wall molecules with random thermal velocities. Although, this model enabled energy transfer between the wall and fluid, it presented difficulties in implementations of moving boundaries.

A more advanced wall model utilizes a lattice of molecules connected to crystal positions with harmonic bonding. Ceiplak et al. (2001) examined boundary conditions at the wall–fluid interface using harmonic springs attached to the lattice position of each wall molecule, which allowed the wall molecules to vibrate, emulating the thermal motion of solid crystals. In order to confine the displacements of the oscillating wall molecules, the authors used high stiffness constants for bonding (Cieplak et al.

2001). Though this represents a remarkable advance to model the wall lattice fluid interactions, a thermostat was deemed necessary to maintain the fluid temperature in equilibrium (Cieplak et al. 2001; Koplik and Banavar 2006). Thermal equilibrium state of the fluid was readily and *uniformly* maintained through the application of thermostat, which dissipated heat due to viscous heating to the imaginary heat reservoir, instead of through the collision/interaction with the neighboring walls. Hence, the thermal interactions between the fluid and surfaces which may have distance dependence through the fluid system were not modeled adequately.

In order to properly consider the nature of thermal transport at the wall–fluid interface, we used the lattice wall model with a characteristic bonding stiffness. Thermal oscillations of wall molecules influence the fluid by absorbing or supplying momentum and energy to fluid molecules via intermolecular interactions. We utilized walls as heat baths to maintain thermal equilibrium of the fluid, therefore there was no need to apply a thermostat uniformly to the equations of motion for the fluid molecules to maintain the system at constant temperature during simulations. Thermal "natural" interactions between the fluid and wall maintained the thermal equilibrium of the fluid, while the temperature of the wall was kept constant. In the case of shear driven flow, energy imparted on the fluid (i.e., work done by the moving wall) was dissipated by the fluid as viscous heating, while constant wall temperature applied on the surface enabled heat loss through the walls.

This paper is organized as follows. We first summarize the theoretical background of the MD method, followed by the shear-driven flow simulation using fixed lattice crystal boundaries for code verification purposes. Section 2 presents the interactive thermal wall model with MD results for shear driven flow. In Sect. 3, we present the effects of crystal bond stiffness on temperature jump. This is followed by the unsteady MD simulations of freezing of liquid argon in a nano-channel. Finally, summary of our findings and conclusions are presented.

2 Simulation method and numerical model

In order to investigate boundary slip in fluid–wall interface, we performed two-dimensional MD simulations for shear driven flow in a 5 nm width channel. For interatomic interactions we employed the most commonly used and simple interaction potential, namely the Lennard–Jones 12–6 potential. The form of Lennard–Jones 12–6 potential is $V(r_{ij}) = 4\varepsilon\left[\left(\frac{\sigma}{r_{ij}}\right)^{12} - \left(\frac{\sigma}{r_{ij}}\right)^{6}\right]$, where ε is the binding energy (depth of the potential) and σ is the molecular diameter (the distance at which the interparticle potential is 0). The first term represents the short-range repulsive interactions preventing the overlap of the molecules, while the second term represents a dipole-induced attractive interaction. The interaction force is between a pair is given by $F_{ij}(r_{ij}) = -\frac{\partial V(r_{ij})}{\partial r_{ij}}$. The temperature of the simulation was set to 120 K, and the number density (N/σ^2) of the system is $\rho = 0.8$, which corresponded to the liquid state of argon (Thompson and Robbins 1990). The temperature in a two-dimensional N particle system can be defined through the average kinetic energy as $\left\langle \sum_i \frac{m_i v_i^2}{2} \right\rangle = \frac{dNkT}{2}$. For argon molecule molecular mass is $m = 6.69 \times 10^{-26}$ kg, molecular diameter is $\sigma = 0.34$ nm and binding energy ε is $119.8 \times k_b$ (1.6539×10^{-21} J). Intermolecular interaction forces were truncated to zero at a cut-off distance of 1.0 nm, which is approximately at 3σ. The top and bottom surfaces were moved in opposite directions with the speed of $U_w = 0.5\sqrt{\varepsilon/m}$ as shown in Fig. 1. Characteristic time $\tau = \sigma\sqrt{m/\varepsilon}$ is 2.16×10^{-12} s, and the simulations used 4 fs ($\sim 0.002\tau$) time steps. Periodicity boundary conditions were imposed in the streamwise direction as described in (Allen and Tildesley 1989). For computational simplicity two-dimensional MD simulations were performed. A total of 313 fluid molecules ($N_f = 313$) were simulated in a two-dimensional 5 nm width channel. For establishing the baseline for our approach and testing the

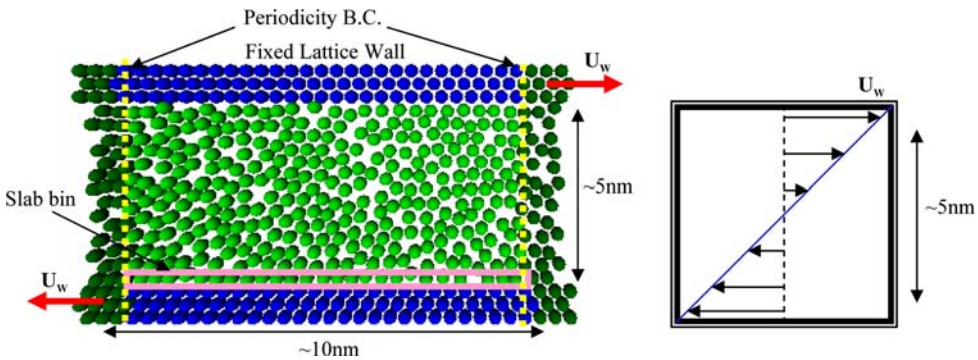

Fig. 1 Schematics of shear driven flow in a 5-nm wide channel. Model contained 313 fluid molecules with fixed lattice crystal walls at moving at a shear rate $\dot{\gamma} = 3.14 \times 10^{10}\text{s}^{-1}$. *Shaded molecules* outside the box in periodic boundary directions are the images of fluid mapped using periodic boundary condition over the domain of interaction

code, we first applied the fixed lattice wall model. Since the walls were modeled as perfectly elastic fixed lattice crystals, there is no heat transfer to/from the walls (Thompson and Robbins 1990). Under such unrealistic thermal interface model, the temperature of the system steadily increases if any kind of work is done on the system. Therefore, it is necessary to dissipate work done by the moving wall using a thermostat (Nose–Hoover). In this thermalized wall model, the temperature of the fluid is maintained around 120 K, as desired. However, thermal transport at the fluid–wall interface has no physical meaning.

Before, we present simulation results with new simulation set up, which utilize the interactive thermal wall model, it is important to reproduce and compare the results at similar conditions with previous MD simulations that utilized fixed lattice crystal walls. Figure 2 shows comparisons of the velocity profiles obtained from our MD simulations and the results in (Thompson and Robbins 1990) for fluid and wall interaction potential strengths of $\varepsilon_{wf} = 0.4\varepsilon$, 1ε and 4. The simulations started from Maxwell to Boltzmann velocity distribution, and ran 1.2×10^6 time-steps (4.8 ns) to reach the steady state, after which, another 1.2×10^6 timesteps were performed for time averaging. Longer time averaging has also been performed to confirm convergence of local velocity and temperature to steady state. The computations with the fixed lattice crystal wall cases are presented only for code verification purposes, where the fluid temperature is maintained a constant using Nose–Hoover thermostat (Evans and Holian 1985). The velocity profiles obtained from fixed lattice wall cases match the results in (Thompson and Robbins 1990), which predict the same velocity-stick and velocity-slip behavior.

Prior to the presentation of the temperature profiles, it is important to demonstrate local thermal equilibrium in the system. Local temperature can be defined only if local thermal equilibrium is established. Using MD simulations with stochastic thermal walls and by applying a thermal gradient, Tenenbaum calculated density and temperature profiles in a nano channel, and demonstrated local thermal equilibrium by comparisons with the predictions of an equation of state (Tenenbaum 1983). Another methodology for verification of local thermal equilibrium is calculation of the higher moments of velocity. At equilibrium, the velocity distribution at the point of measure should have normal (Gaussian) distribution with zero skewness and kurtosis. For *all cases* presented in this paper, we calculated higher moments of the velocity distribution for the first slab bin adjacent to the bottom wall and for a bin at the channel center. The results have shown almost normal distribution of the velocity with skewness and kurtosis varying between −0.097 to 0.054 and −0.092 to 0.202, respectively. Therefore local thermal equilibrium in the fluid was maintained for all of our simulations. For steady results, the ensemble was collected at every fifth time-step for 25,000 time-steps (100 ps) to obtain a reasonable ensemble average. For the transient (freezing) case, shorter collection time (5,000 time-steps, 20 ps) was used to present temperature distribution at 20 ps intervals. As a result, kurtosis of the transient case was slightly larger (−0.092 to 0.202) than the steady state cases (0.012–0.023).

2.1 Thermal walls interacting with fluid molecules

In order to properly implement thermal interactions between the fluid and wall molecules, we utilized lattice bond springs as described in Cieplak et al. (2001) and Koplik and Banavar (2006), which were attached to the wall molecules at their lattice positions. Moreover, we included more advanced thermal interaction mechanisms to the walls. For initial conditions, the velocities for thermal oscillations were assigned from a Maxwell–Boltzmann distribution consistent with the target temperature, and then the thermostat was applied to wall molecules to absorb/supply heat from/to the fluid via wall/fluid interactions.

Previous nanoscale MD simulations defined important features of the boundary slip on nanoscale fluid flows as

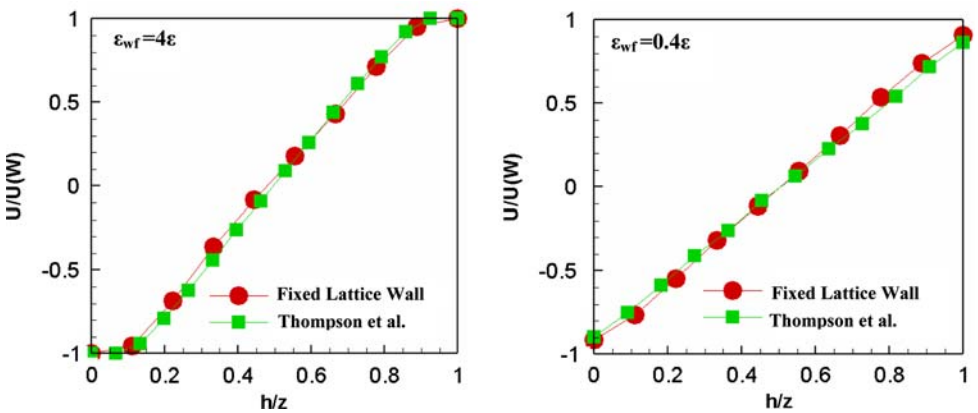

Fig. 2 Velocity slip/stick on the walls at various liquid/wall interaction strengths. Comparison is made with the results obtained by Thompson and Robbins(1990)

function of the strength of wall/fluid interactions, the density of fluid and the shear rate. However, their results did not properly include thermal interactions between wall and fluid. In order to improve this, our interactive thermal wall model has its own thermal oscillations and it exchanges momentum and energy between fluid and the wall. Therefore, excessive heat in the fluid is transferred to the walls, and then, the heat is dissipated through the thermostat applied on the walls.

We use the velocity Verlet algorithm for time integration (Allen and Tildesley 1989). In order to find the position and velocity of molecules at the next time step, evaluation of intermolecular forces are required. Detailed forces of interactions experienced by each of the fluid molecule and wall molecules are calculated separately by using interaction potentials between fluid molecules and fluid molecules and wall molecules. The total force experienced by a fluid molecule is therefore a sum of these two terms:

$$F_{\text{fluid}}(r_i) = \sum_{j=1}^{N_f} \frac{\partial V(r_{ij})_{\text{fluid-fluid}}}{\partial r_{ij}} + \sum_{j=1}^{N_w} \frac{\partial V(r_{ij})_{\text{fluid-wall}}}{\partial r_{ij}}. \quad (1)$$

Every fluid molecule interacts with other fluid or wall molecules within the predetermined cutoff distance. The forces depend on interparticle distances. Hence, thermal oscillations of wall molecules affect the forces acting on the fluid molecules through this variation of their position as well. In order to properly implement the thermal interactions between fluid and wall molecules properly, the forces due to fluid molecules on the motion of wall molecules must be taken into account while reducing the interactions between molecules of wall to a crystal bond-stiffness and defining each as independent oscillators. The resulting force on a molecule of the wall is given as

$$F_{\text{wall}}(r_i) = \sum_{j=1}^{N_f} \frac{\partial V(r_{ij})_{\text{wall-fluid}}}{\partial r_{ij}} + K(|r_0 - r_i|), \quad (2)$$

where K is the wall crystal bonding stiffness and $|r_0 - r_i|$ is the distance between the original lattice position and current position of the wall molecule. Equation (1) is the force exerted on a fluid molecule by the surrounding fluid and wall molecules, while Eq. (2) is the force exerted on a wall molecule by fluid molecules and the attached lattice springs. The ideal way of constructing a wall as a heat reservoir is to form thermally oscillating crystals with an infinite number of molecules, and then make those wall molecules interact with each other. However, including interactions between very large numbers of wall molecules are computationally prohibitive. Moreover, our focus was not on the thermal behavior of solid walls but the proper characterization of thermal interactions of fluid molecules with the wall. Therefore, it is most efficient to construct interactive thermal walls without including the N_w^2 interactions between the wall molecules while maintaining physics. For the interactive thermal wall model, we applied velocity scaling thermostat to each wall layer separately with parameter $\eta_{\text{layer}} = \sqrt{\frac{T_{\text{assigned-wall}}}{T_{\text{layer-wall}}}}$ at every time step. Since there were no interactions between the crystal layers, these scaling surrogate the thermal interactions between the layers of lattice wall crystals, and keeps all layers at a prescribed temperature. For initial conditions, interactive thermal walls have thermal oscillations described by the Boltzmann velocity distribution at a desired temperature. As the simulation proceeds, thermal oscillations of wall molecules are affected from wall/fluid interactions, which enable heat transfer from fluid to the wall. Since wall molecules do not interact with each other, cut off distance of 1 nm is enough for the thickness of the wall modeled using three layers of wall molecules, and the thermostat should be applied to each layer of the lattice crystal molecules separately, as shown in Fig. 3. Otherwise, the first layer (surface) of the wall, which adjoins to the fluid, would have most of the thermal velocity distribution, and a relatively high temperature as compared to the average

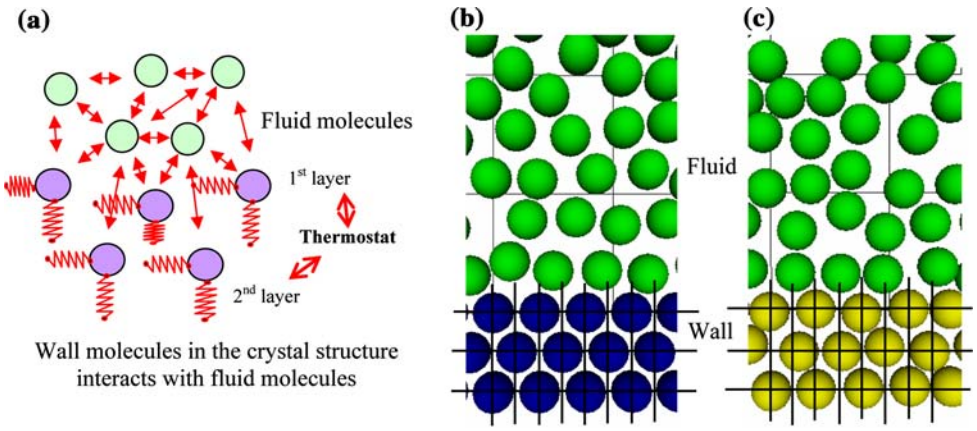

Fig. 3 **a** Schematics representation of thermal wall–fluid interactions using a crystal bond spring attaches the molecules to their lattice positions; **b** Wall molecules fixed in a lattice position; **c** a snapshot of the wall molecules in thermal oscillations (deviated from their lattice position) interacting with fluid molecules

wall temperature. In comparison to the ideal "all atom-all interacting" wall case that requires additional N_w^2 operations to properly exchange heat with the fluid, our thermal wall model is computationally cheap, and yet it is as effective as the ideal wall model. Moreover, by applying thermostats to each layer of the wall, there is no omission of thermal interactions between fluid/wall molecules. Therefore, viscous heating is dissipated thorough the isothermal walls.

Shear driven nano-flow simulations with same configuration to that in Fig. 2 are repeated using the new interactive thermal wall model utilizing crystal bonding stiffness of $K = 64\left(4\varepsilon_{gas}/\sigma^2\right)$. The velocity profiles obtained from the new thermal model are compared with the fixed lattice wall model in Fig. 4. Velocity profiles predicted by both models are similar to each other. However, there are significant differences between the two models in the prediction of temperature profile. Work done by the shearing of walls induces viscous heating to the fluid, while the system reaches to steady state by heat dissipation through the walls. As a result, temperature distribution in the fluid shows parabolic profiles with a jump at the wall/fluid interface (Fig. 5). Parabolic temperature distribution is expected, since the shear rate is a constant in the entire domain, which not only results in a linear velocity profile, but also a constant heating rate. Surprisingly this behavior is observationally similar to that of rarefied gas flow in shear-driven micro-channel, which exhibits a linear velocity profile with slip, and a parabolic temperature distribution with jumps (Karniadakis et al. 2005). Despite these similarities, physical reasons for these jumps are different between gas and liquid flows.

Different thermal oscillation frequencies of two dissimilar materials induce a thermal resistance at their interface. Thermal resistance of metal/liquid–helium interface was first discovered by Kapitza (1941), and it is also known as the Kapitza resistance (Kapitza 1941). The classical theory to explain heat transfer between solid/liquid interfaces basically assumes the thermal resistance on the interface to essentially depend on the phonon density, which determines the heat transmission ratio between the two dissimilar materials (Pollack 1969). However a recent MD study has shown that surface wettability (i.e., wall/fluid interaction strength) also enhanced the heat transmission ratio on the solid/liquid interface (Barrat and Chiaruttini 2003). Figure 5 shows how the wall/fluid interaction strength (surface wettability) in the shear flow affects the interface temperature jump while it causes velocity locking or slip of the fluid. Moreover, for strong attractive walls, MD studies have shown layering effects of the liquid molecules next to the surface and the layered structure went through a transition as the interaction strength changes (Chaudhuri et al. 2007), and the structural changes of the layered molecules also changes thermal conductance at the interface (Chaudhuri and Dhar 2006). Our results in Fig. 5 show temperature jump being a function of the wall/fluid interaction strength, which results in different thermal (Kapitza) resistance on the interface. Strong interactive forces reduce both the temperature jumps and velocity slip at the interface. However, the fixed lattice model, which applies the Nose–Hoover thermostat on the fluid, shows almost uniform temperature

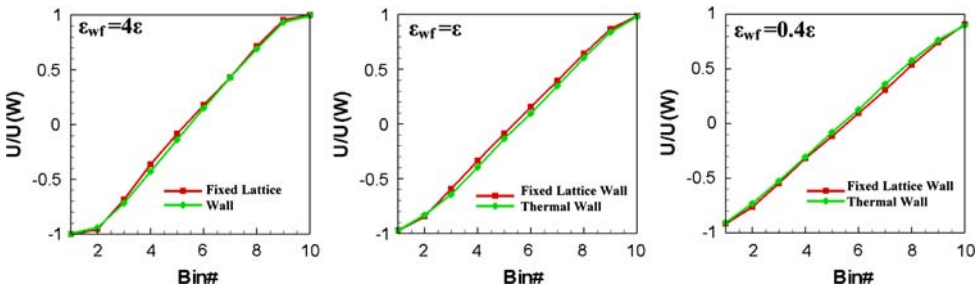

Fig. 4 Velocity profiles resulted in shear-driven flow simulations with interactive thermal wall model and fixed lattice crystal walls

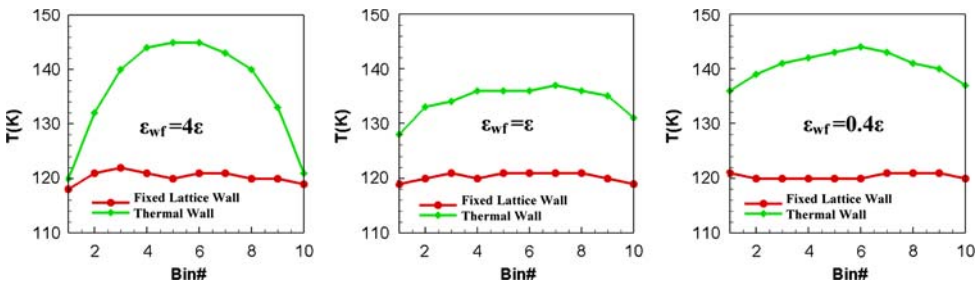

Fig. 5 Temperature profiles resulted in simulations with fixed lattice crystal wall model and with the interactive thermal wall model at various wall/fluid interaction strengths

distribution. Therefore, thermal interactions between the fluid and wall predicted by the fixed lattice wall model are unphysical. In order to investigate further for the effects of thermal oscillation frequency, heat transfer MD simulations with two different crystal bonding stiffness are presented in the next chapter.

3 Temperature jumps on high crystal bond stiffness

Previously, Thompson and Troian have investigated velocity slip on the boundary as functions of the wall/fluid interaction potential strength, wall density and shear rate (Thompson and Troian 1997). As shown in the previous section, the interactive thermal wall shows similar velocity slip results with the fixed lattice wall model. However, the temperature profiles inside the channel are significantly different. Moreover, a temperature jump is observed at the boundary when the wall/fluid interaction potential is weak. The temperature jump at the boundary is caused by fluid molecules near the wall boundary that have different thermal velocity from the wall. Since the local temperature of a system defined through the thermal velocities of molecules, effective momentum transfer between the wall and fluid is important. If the wall/fluid interactions are weaker or less effective than the fluid/fluid interactions, it is obvious that the thermal motions of fluid molecules are more dominantly influenced by the neighboring molecules of fluid rather than the neighboring wall molecules. Therefore, weak wall/fluid interactions generate a momentum deficit at the wall/fluid interface. This causes sudden changes in distribution of local kinetic energy, which is directly related to the temperature jump at the interface. Therefore, it is obvious that, when there are strong wall/fluid molecular interactions, there is no temperature jump as shown in Fig. 5a. Density also plays an important role because the more dense the system is, there is more opportunity for the interactions between the wall and fluid molecules.

Crystal bonding stiffness constant K, is an additional parameter for the wall/fluid interface that has an affect on the temperature jump. For a simple harmonic oscillating system with constant total energy, stiffness of the system determines the oscillation frequency, the amplitude is mainly determined by the temperature of wall (but the anharmonicity induced by the interactions between wall and fluid molecules becomes more dominant if K is soft, hence larger amplitude motion may result). Since the temperature is measured through time averaged kinetic energy, different bond stiffness generates different kinetic energy fluctuations; still the averages of the kinetic energy are the same. Therefore, for walls at the same temperature, larger crystal bonding stiffness generates higher frequency

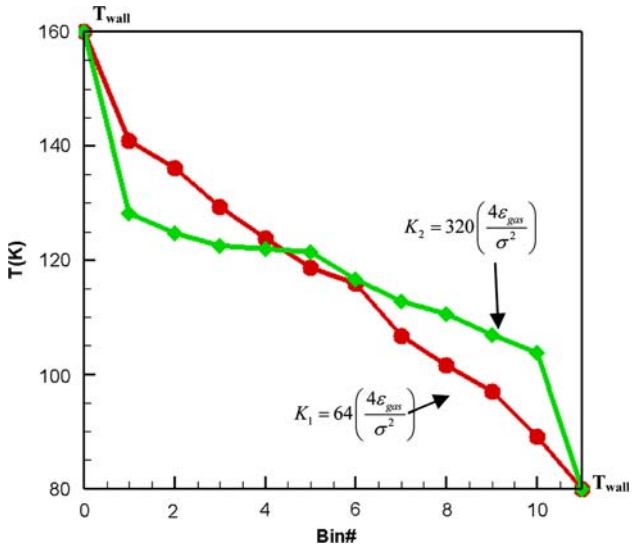

Fig. 6 Temperature profile dependence (over the 10 slabs -each with 1 nm thickness, channel width 10 nm) on different crystal bonding stiffness values ($K_2 = 5\ K_1$)

thermal oscillations with smaller deviations from the temperature dictated amplitudes. In order to investigate further the relation between the temperature jump and the crystal bonding stiffness, two nanoscale heat transfer MD simulations were performed by using different bonding stiffness constants, K in Eq. (2). We should point out that we determine these two different crystal bonding stiffness constants K_1 and K_2 from the second derivative of the Lennard–Jones potential for wall molecules for the distance where pairwise energy is minimum. This corresponds to the curvature of the potential well; here K_2 is five times larger than K_1. The distance between the walls is taken as 10 nm, $\varepsilon_{wf} = \varepsilon$ and number density is $\rho = 0.8$. Temperature at the bottom and top walls is 80 and 160 K, respectively. Figure 6 shows that the temperature jump was observed at large stiffness $\left(K_2 = 320\left(4\varepsilon_{gas}/\sigma^2\right)\right)$ values; however, at $K_1 = 64\left(4\varepsilon_{gas}/\sigma^2\right)$, compliant with the thermal oscillation of fluid molecules at density $\rho = 0.8$, there was no temperature jump. This shows the importance of the crystal bonding stiffness K for thermal equilibrium at the liquid/solid interface. Thermal equilibrium at the interface also depends on the effectiveness of momentum transfer between the wall and fluid molecules and their impact on thermal oscillations of the molecules of walls. Figures 5 and 6 show that at low fluid densities, weak wall/fluid interaction potential as well as large crystal bonding stiffness provide less effective momentum transfer between the wall and liquid molecules, and results in larger Kapitza resistance. Increased Kapitza resistance on the interface shows deviation in the local kinetic energy distribution and results in temperature jumps at the wall/liquid interface.

4 Transient heat transfer simulations

In this section, MD simulation results for a transient heat transfer problem are presented. Initially, the simulation domain has a 10 nm distance between the walls, and the temperature for interactive thermal walls $\left(K_1 = 64\left(4\varepsilon_{\text{gas}}/\sigma^2\right),\ \varepsilon_{\text{wf}} = \varepsilon\right)$ and argon fluid molecules ($\rho = 0.8$) was set to 200 K. Periodic boundary condition was applied in the streamwise direction. From the equilibrium state at 200 K, the wall temperature was suddenly dropped to 20 K using the thermostats. Naturally, the wall started absorbing heat from the liquid. Due to heat transfer through the wall, thermal motions of liquid molecules are slow down as they moved to lower energy states in configuration space as well. Hence, the liquid molecules near the wall started to crystallize (freeze) as shown in Fig. 7a. Figure 7b shows the number density fluctuation of fluid molecules in each of the slab bins between the walls. Each slab bin has a width of 0.1 nm and a length of 10 nm. This density fluctuation ($\rho_{\text{bin}} - \rho_{\text{avg}}$) shows layering of fluid molecules as it crystallizes. Moreover, the figure enables us to observe the process of crystallization. At earlier times, the liquid region shows limited density fluctuations along the width of the channel, because the molecules can freely move in the liquid state. However, in the case of crystallized molecules, the number density fluctuates across the channel as shown at 400–420 ps time frames in Fig. 7b.

Figure 8 shows the transient local temperature of the initially hot (200 K) liquid between two cold (at $T = 20$ K) walls during the cooling process. Each of the temperature profile was averaged for 20 ps to smooth out the statistical fluctuations. The liquid temperature reaches the equilibrium state temperature of 20 K after 400 ps. However, temperature of the wall and fluid are different at the beginning of the cooling process, even though the wall ($\varepsilon_{\text{wf}} = \varepsilon$) had compliant crystal bonding stiffness (K_1). This result is significantly different than the continuum theory that predicts the same temperature at the interface.

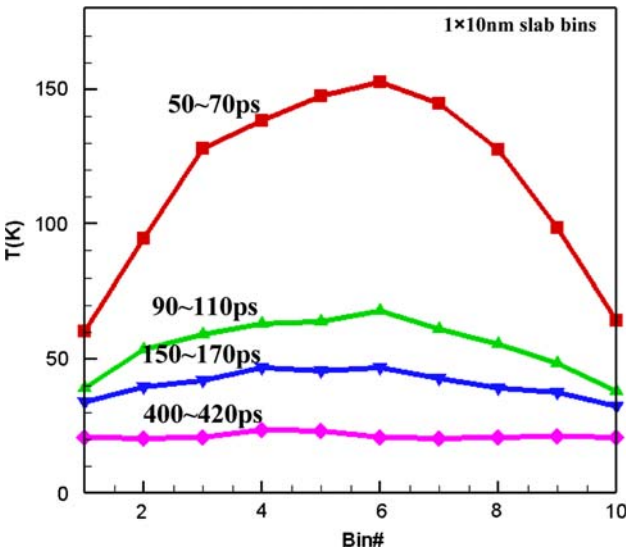

Fig. 8 Temperature distribution at various times for the freezing process shown in Fig. 7

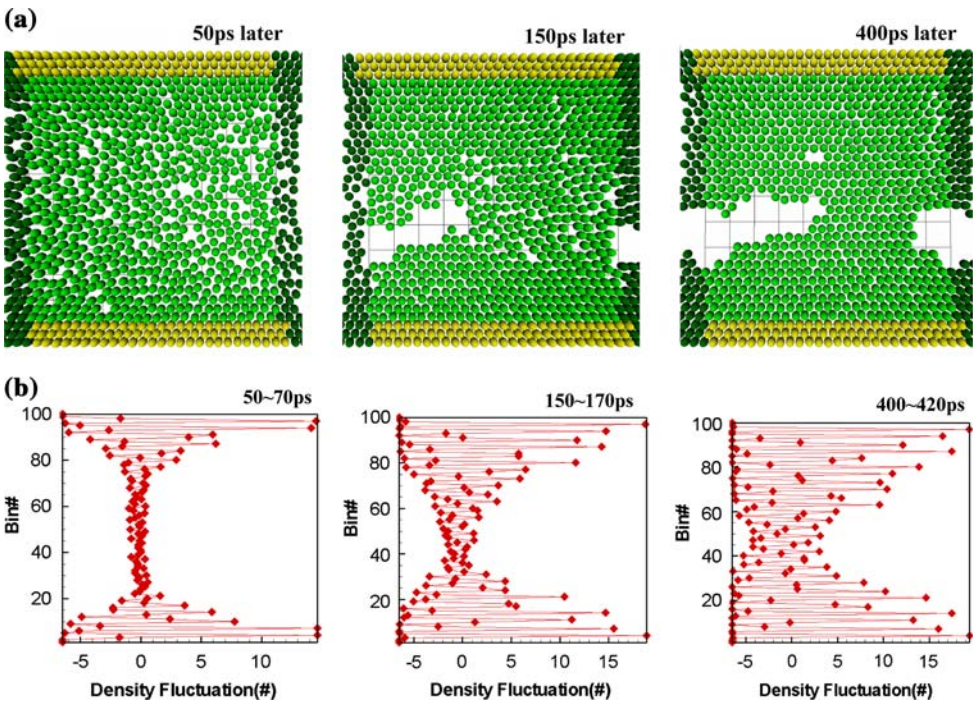

Fig. 7 Freezing process of argon, initially at 200 K and in contact with two walls at 20 K **a**. Density fluctuations ($\rho_{\text{bin}} - \rho_{\text{avg}}$) in 0.1 × 10 nm slab bins as a function of time **b**

5 Conclusions

In this study, nanoscale MD simulations of thermally interacting fluid/wall interfaces are presented. Previous MD simulations were mostly focused on the velocity slip on the boundary. For the velocity slip on boundary, interaction potential strength, shear rate and density of wall molecules were the most important properties, as elucidated by previous MD simulations. However, we present a more realistic interactive thermal wall model that allows thermal interactions between the fluid and wall. The result shows that strong interactions between the wall and fluid molecules result in no temperature jumps on the interface. On the contrary, when the interaction potential is weak or the wall has a large crystal bonding stiffness, temperature jumps on the wall/fluid interface are observed. These new results show that the temperature distribution near the boundary is not only affected by the fluid density or strength of interaction potential, but it also strongly depends on the crystal bonding stiffness of wall molecules. In conclusion, crystal bonding stiffness, density and the interaction strength are key parameters for temperature jump on the solid/liquid interface.

References

Allen MP, Tildesley DJ (1989) computer simulation of liquids, Oxford University Press, Oxford

Andersen HC (1980) Molecular dynamics simulations at constant pressure and/or temperature. J Chem Phys V72(4):2384–2393

Barrat J-L, Chiaruttini F (2003) Kapitza resistance at the liquid–solid interface. Mol Phys V101(N11):1605–1610

Berendsen HJC, Postma JPM, van Gunsteren WF, DiNola A, Haak JR (1984) Molecular dynamics with coupling to external bath. J Chem Phys V81(8):3684–3690

Bird GA (1994) Molecular gas dynamics and the direct simulation of gas flows. Oxford University Press, Oxford

Chaudhuri D, Dhar A (2006) Heat conduction in a confined solid strip: response to external strain. Phys Rev E 74:016114

Chaudhuri D, Chaudhuri A, Sengupta S (2007) Heat conduction through a trapped solid: the effect of structural changes on the thermal conductance. J Phys Condens Matt V19:152201

Cieplak M, Koplik J, Banavar JR (1999) Application of statistical mechanics in subcontinuum fluid dynamics. Physica A 274:281

Cieplak M, Koplik J, Banavar JR (2000) Molecular dynamics of flows in the Knudsen regime. Phys A 287:153–160

Cieplak M, Koplik J, Banavar JR (2001) Boundary conditions at a fluid–solid interface. Phys Rev Lett V86:N5

Evans DJ, Holian BL (1985) The Nose–Hoover thermostat. J Chem Phys V83:4069–4074

Evans DJ, Hoover WG (1986) Flows far from equilibrium via molecular dynamics. Annu Rev Fluid Mech V18:243–264

Hoover WG (1985) Canonical dynamics: equilibrium phase–space distributions. Phys Rev A V31:1695–1697

Kapitza PL (1941) Zh Eksp Theor Fiz 11 1. J Phys USSR V4:181

Karniadakis GE, Beskok A, Aluru N (2005) Microflows and nanoflows: fundamentals and simulation. Springer, Heidelberg

Koplik J, Banavar JR (1995) Continuum deductions from molecular hydrodynamics. Annu Rev Fluid Mech V27:257–292

Koplik J, Banavar JR (2006) Slip, immiscibility, and boundary conditions at the liquid–liquid interface. Phys Rev Lett V96:044505

Koplik J, Banavar JR, Willemsen JF (1989) Molecular dynamics of fluid flow at solid surfaces. Phys Fluids A V1:781–794

Maxwell JC (1879) On stress in rarefied gases arising from inequalities of temperature. Philos Trans R Soc Lon V170:231–256

Nose S (1984) A unified formulation of the constant temperature molecular dynamics methods. J Chem Phys V81:511–519

Nose S (2002) A molecular dynamics method for simulations in the canonical ensemble. Mol Phys V100:191–198

Pollack GL (1969) Kapitza resistance. Rev Modern Phys V41(N1):48–81

Priezjev NV, Darhuber AA, Troian SM (2005) Slip behavior in liquid films on surfaces of patterned wettability: comparison between continuum and molecular dynamics simulations. Phy Rev E 71:041608

Sun M, Ebner C (1992a) Molecular-dynamics simulation of compressible fluid flow in two-dimensional channels. Phys Rev A V46:4813–1818

Sun M, Ebner C (1992b) Molecular dynamics study of flow at a fluid–wall interface. Phys Rev Lett V69:N24

Tenenbaum A (1983) Local equilibrium in stationary states by molecular dynamics. Phy Rev A V28(N5):3132–3133

Thompson PA, Robbins MO (1990) Shear flow near solids: epitaxial order and flow boundary conditions. Phys Rev A 41(V41):6830

Thompson PA, Troian SM (1997) A general boundary condition for liquid flow at solid surfaces. Nature V389(6649):360